Plant Biotechnology 31, 149–158 (2014)
DOI: 10.5511/plantbiotechnology.14.0204a

Original Paper

Regulatory change in cell division activity and genetic mapping of a tomato (*Solanum lycopersicum* L.) elongated-fruit mutant

Katarut Chusreeaeom[1], Tohru Ariizumi[1], Erika Asamizu[2], Yoshihiro Okabe[1], Kenta Shirasawa[2], Hiroshi Ezura[1,*]

[1]Graduate School of Life and Environmental Sciences, University of Tsukuba, Tsukuba, Ibaraki 305-8572, Japan; [2]Kazusa DNA Research Institute, Kisarazu, Chiba 292-0818, Japan
*E-mail: ezura@gene.tsukuba.ac.jp Tel & Fax: +81-29-853-7263

Received January 16, 2014; accepted February 4, 2014 (Edited by T. Mizoguchi)

Abstract Tomato elongated-fruit mutants have proven useful for elucidation and mapping of genes that regulate fruit elongation. We previously identified a novel tomato mutant, *Solanum lycopersicum elongated fruit1* (*Slelf1*), which exhibits an elongated fruit shape caused by increased cell layers in the ovary proximal region, and located the causal genes on the long arm of chromosome 8. In this study, we isolated and characterized two independent tomato mutants, *Solanum lycopersicum elongated fruit2* and *3* (*Slelf2* and *Slelf3*). Histological analysis revealed that the *Slelf2* mutant ovary displayed an overall elongated shape, whereas the developing ovary of the *Slelf3* mutant was primarily expanded in the proximal region. We developed an intra-specific F_2 population by crossing *Slelf3* with Ailsa Craig, a related cultivar. Mapping of this population confirmed that the candidate gene of the *Slelf3* mutation was positioned on the short arm of chromosome 7, in a region of approximately 0.4 Mb. These results indicate that the causal gene is a novel locus differing from previous genes known to affect fruit shape elongation in tomatoes. In addition, analysis of transcript levels of genes related to cell division and expansion in the *Slelf3* mutant suggested that the mutated gene most likely regulates cell division activity, predominantly in the proximal region.

Key words: Tomato (*Solanum lycopersicum* L.), cell division, genetic mapping, fruit shape, tomato mutant.

Tomato (*Solanum lycopersicum* L.) is an economically important food crop. It is also an ideal dicot model species to investigate various physiological phenomena because of its relatively compact genome (950 Mb) and diploid status ($2n=2x=24$), and the availability of a marker-saturated genetic linkage map and rich germplasm collections (Tomato Genetics Resource Center). Major fruit quality characteristics of interest to both the tomato-processing industry and fresh market include fruit size and shape. Elongated tomato fruit is one of the most persistence shape, and are widely used for processing because their shape is more convenient for mechanical harvesting and a better fit in cans than round tomatoes. The elongated fruit shape is also considered desirable for fresh consumption. In spite of this popularity, however, the molecular basis of fruit shape elongation is not well understood. The International Tomato Sequencing Project, established in 2004, promotes structural genome analysis of tomato via sequencing of all 12 chromosomes. Data are published predominantly through the SOL Genomics Network (SGN) website (http://solgenomics.net/; Mueller et al. 2005), with three DNA marker types currently developed: expressed sequence tag (EST)-derived simple sequence repeat (SSR) markers (TES markers), genome-derived SSR markers (TGS markers), and EST-derived intronic polymorphism markers (TEI markers). In a recent study (Shirasawa et al. 2010), ratios of screened polymorphisms were used to genotype a Tomato-EXPEN 2000 mapping population and construct a high-density genetic linkage map, composed of 1,433 new and 683 existing marker loci covering 1,503.1 cM across the 12 tomato chromosomes. Information on these DNA markers is available at http://www.kazusa.or.jp/tomato/.

The conveniently sized, dwarf tomato variety Micro-Tom, which can be densely planted in large-scale

Abbreviations: AC, Ailsa Craig; CAPS, Cleaved Amplified Polymorphic Sequences; DAF, days after flowering; DAP, days after planting; dCAPs, derived Cleaved Amplified Polymorphic Sequence; EMS, ethylmethane sulfonate; NBRP, National Bioresource Project; *Slelf1*, *Solanum lycopersicum elongated fruit 1*; SSR markers, simple sequence repeat markers; TES markers, *tomato* expressed sequence tag (EST)-derived SSR markers; TGS marker, *tomato* genome-derived SSR markers; WT, wild type.

This article can be found at http://www.jspcmb.jp/
Published online May 28, 2014

cultivation, has been widely used for functional genomics studies. Taking advantage of Micro-Tom's rapid life cycle and the existence of functional genomics tools, a genetic map with DNA markers and a mutant database have been generated for this variety (Saito et al. 2011; Shirasawa et al. 2010). Additionally, ESTs and full-length cDNAs of Micro-Tom have been published at MiBASE (http://www.kazusa.or.jp/jsol/microtom/) and KafTom (http://www.pgb.kazusa.or.jp/kaftom/) (Yamamoto et al. 2005).

At the University of Tsukuba, researchers have identified 1,819 phenotypic categories in 1,048 mutants produced in the background of Micro-Tom by ethylmethane sulfonate (EMS) mutagenesis and gamma-ray irradiation (Saito et al. 2011). We have also identified and characterized a novel tomato mutant, *Solanum lycopersicum elongated fruit1* (*Slelf1*), exhibiting an elongated fruit shape caused by increased cell layers in the ovary proximal region and controlled by genes located on the long arm of chromosome 8. These mutant resources are available through the National BioResource Project Tomato TOMATOMA database (http://tomatoma.nbrp.jp/).

SUN and *OVATE*, the two major genes stimulating elongated fruit structure, are among those associated with tomato mutations responsible for homeotic transformation of fruit shape (Liu et al. 2002; Xiao et al. 2008). The *SUN* gene encodes an IQ67 domain-containing protein, with 33 and 29 members of this gene family predicted in *Arabidopsis* and rice, respectively. *SUN* gene duplication has been revealed to promote fruit elongation in tomato, and 34 *SlSUN* homologs have been identified (Huang et al. 2013). A mutation in *OVATE*, a gene encoding an OVATE family protein (OFP), results in the transformation of tomato fruit from round to pear-shaped. Huang et al. (2013) reported the presence of 31 *SlOFP* gene homologs in tomato and identified their positions on 12 chromosomes. These homologs were found to be enriched on the top and bottom segments of several chromosomes.

Early tomato fruit development involves fundamental cellular processes such as cell division and cell expansion phenomena. Cyclin-dependent protein kinases (CDKs) are major regulators of cell cycle progression and play a crucial controlling role in cell division (Inze and De Veylder 2006). Plant cyclins are currently classified into five major groups (A–D and F), with A- and B-type *CDKs* the most prominent and numerous. Only a few mutants with altered *CDKB* expression have been reported. In *Arabidopsis*, changes in CDKB protein activity lead to various meristematic defects (Andersen et al. 2008). In tomato, *CDKB1.1* and *CDKB2.1* are the only *CDKBs* presently identified (Chevalier 2007); overexpression of these B-type *CDK* genes results in smaller cells and fewer cell layers in the pericarp (Czerednik et al. 2012). Another class of proteins associated with early fruit development are expansins, which are plant cell-wall loosening proteins involved in cell enlargement (cell expansion). Four families of expansins from the largest, most well-known plant largest families have been recognized and described: α-expansin (EXPA), β-expansin (EXPB), expasin-like A (EXLA), and expansin-like B (EXLB) (Sampedro and Cosgrove 2005).

In this paper, we report the isolation and characterization of two elongated-fruit mutants, *Solanum lycopersicum elongated fruit 2* and *3* (*Slelf2* and *Slelf3*). Although the ovary of the *Slelf2* mutant exhibited an overall elongated shape, its proximal region was shown at 10 days after flowering (DAF) to be the key elongated region of this mutant. In addition, we found that the *Slelf3* mutant phenotype was caused by regulation of cell division activity through stimulated elongation of ovary and fruit, particularly in the proximal region; pericarp thickness and the number of cell layers were both increased primarily in this area. To gain deeper insights into genetic control of fruit elongation, rough mapping of a *Slelf3* F_2 population—from a cross between *Slelf3* and the related cultivar Ailsa Craig, was also performed.

Materials and methods

Plant materials and phenotypic measurements

Tomato (*S. lycopersicum* L.) long-fruit mutant lines TOMJPE2407 and TOMJPE839, herein named *Slelf2* (*S. lycopersicum elongated fruit2*) and *Slelf3* (*S. lycopersicum elongated fruit3*), respectively, had been previously generated in the background of Micro-Tom, a dwarf, rapid-growth variety, by EMS mutagenesis (Saito et al. 2011). The wild-type Micro-Tom and EMS-mutagenized plants were grown on soil in a standard greenhouse. To determine the way in which vegetative and reproductive traits were affected by the *Slelf2* and *Slelf3* mutations, a phenotypic characterization was performed by monitoring parameters related to cotyledon shape, hypocotyl and root length, leaf size and shape, and plant height. Date of flowering was recorded for time-course observation of flower development at −8, −6, −4, −2, 0, and 2 DAF, and fruits at 10 DAF were used for histological analysis. The following components in mature red fruits were measured: length, diameter, fresh weight, locule number, and number of seeds per fruit.

Histological and microscopic analysis

Flower bud tissues at −8, −4, and 0 DAF and fruit at 10 DAF were fixed in FAA (3.7% formaldehyde, 5% acetic acid, and 50% ethanol), vacuum-infiltrated twice for 15 min each, and left overnight. The fixed tissues were dehydrated with *t*-butyl alcohol in a step-wise manner by serial incubation at room temperature in increasing concentrations of *t*-butyl alcohol: 10%, 20%, 35%, 55%, 75%, and 100% unified with 40%, 50%, 50% 45%, and 25% ethanol, respectively. Each incubation step

lasted 4–6 h. The tissues were embedded in paraffin (Paraplast; Sigma-Aldrich, Steinheim, Germany), and then sliced into 10–16-μm sections. Paraplasts were removed with xylene, and the sections were hydrated, stained with 0.1% toluidine blue in sodium phosphate buffer (pH 7.0), and viewed under an Olympus BX53 microscope (Tokyo, Japan). Micrographs were captured using an Olympus DP73 camera at 1,728 dpi. Contrast was adjusted using the Adobe Photoshop CS3 Extended software program (Adobe Systems, California, USA).

Mapping population construction and molecular analysis

To explore gene loci, an F_2 population was constructed from a cross between *S. lycopersicum* 'Ailsa Craig' and the *Slelf3* mutant in the Micro-Tom (wild-type [WT]) background. The *Slelf3* F_2 population, consisting of 128 plants, was grown in the greenhouse during spring 2012. Eight representative fruits were harvested from each plant, sliced longitudinally, and measured for fruit shape index (length/diameter ratio).

Total genomic DNA was isolated from young leaves, frozen in liquid nitrogen, and homogenized with a pestle. Genomic DNA was extracted using a Maxwell 16 Tissue DNA Purification kit (Promega, Tokyo, Japan). Genetic maps were constructed using a combination of TES, TGS, cleaved amplified polymorphic sequence (CAPs), and derived cleaved amplified polymorphic sequence (dCAPs) markers. Additional information on all markers, including map location and primer information, can be found on the Kazusa DNA Research Institute website (http://www.kazusa.or.jp/tomato/). The genetic maps for the *Slelf3* mutant contained 30 markers across the 12 tomato chromosomes.

PCR amplification

PCR conditions used to amplify SSR markers were as follows: 94°C for 3 min as an initial denaturation, followed by three cycles of 94°C for 30 s and 68°C for 30 s, three cycles of 94°C for 30 s and 66°C for 30 s, three cycles of 94°C for 30 s and 64°C for 30 s, three cycles of 94°C for 30 s, 62°C for 30 s, and 72°C for 30 s, three cycles of 94°C for 30 s, 60°C for 30 s, and 72°C for 30 s, three cycles of 94°C for 30 s, 58°C for 30 s, and 72°C for 30 s, three cycles of 94°C for 30 s, 55°C for 30 s, and 72°C for 30 s, and one cycle of 72°C for 10 min. Electrophoresis of the resulting products was performed on a 10% polyacrylamide gel (10% PAGE). The gel was stained with ethidium bromide for visualization. Amplifications of CAPs and dCAPs markers were conducted using the following conditions: an initial 2-min denaturation at 94°C, followed by 40 cycles of 1 min at 94°C, 1 min at 55°C, and 1 min at 72°C, and a 5-min final extension at 72°C. The resulting amplicons were incubated with restriction enzymes for over 4 h.

Statistical analysis

Comparisons between means (ANOVA and Tukey–Kramer HSD test; $p=0.05$) were used to analyze differences between varieties. Data are presented as means±standard error (SE), with a 5% level of significance ($p=0.05$). Chi-squared (χ^2) tests were performed to examine goodness-of-fit between expected and observed Mendelian segregation ratios in mutant populations.

Quantitative real-time PCR

Quantitative real-time PCR (qRT-PCR) was used to examine and quantify expression of cell division- and cell expansion-related genes. For RNA extraction, floral buds were carefully separated into sepals, petals, ovaries, and anthers. Fruit pericarps were divided into three designated areas following histological analysis (Figure 6B). Total RNA was extracted from floral organs, cotyledons, stems, and fruit pericarps using an RNeasy Plant Mini kit (Qiagen, Tokyo, Japan) according to the supplier's instructions. Single-strand cDNA was synthesized from 400 ng of total RNA using a SuperScript VILO cDNA Synthesis kit (Invitrogen, Tokyo, Japan). The qRT-PCR experiments were performed on a Takara Thermal Cycler Dice Real-Time system using SYBR Premix Ex Taq II (Takara, Shiga, Japan) and gene-specific *SlCDKB2.1* forward (5′-ATG CTG GTA AGA GTG TAT CGG-3′) and reverse (5′-CGG AGA GTA GTT GGA GGA AC-3′) primers, and *SlEXPA5* forward (5′-AAG GGT TCA AGA ACT CAA TGG CAA C-3′) and reverse (5′-ACC ATC GCC TGT AGT GAC CTT AAA G-3′) primers. For the PCR amplification, the cDNA was denatured at 94°C for 30 s in the first cycle, followed by 45 cycles of denaturation for 5 s, primer annealing at 55°C for 10 s, and extension at 72°C for 15 s. mRNA levels were determined relative to those of the internal control gene *SAND* (accession no. SGN-U316474) according to the methods of Rodriguez et al. (2008).

Results

Characterization of novel elongated-fruit mutants derived from EMS mutagenesis

Exploiting the small size and rapid life cycle of Micro-Tom, induced mutagenesis by EMS was used to generate *Slelf2* and *Slelf3* mutants in the background of this plant model. In these mutants, obviously elongated fruits were visible beginning in early fruit (EF) development (Figure 1). Hypocotyls and roots were observed 7 days after germination. *Slelf2* and WT Micro-Tom had hypocotyls and roots of comparable length, whereas those of *Slelf3* were significantly shorter (Figure 2A; Table 1). The mutations did not affect the cotyledon structure of either mutant line (Figure 2B), but *Slelf3* exhibited altered leaf morphology. More specifically, WT Micro-Tom leaves usually had five leaflets of similar size and shape, with serrated borders. The *Slelf2* mutant produced leaves of comparable morphology to those of the WT, but the mutation in the *Slelf3* line resulted in reduced leaf lobing and decreased leaf area compared with the WT (Figure 2C; Table 1). Plant heights of *Slelf2* and *Slelf3* at 30 days after planting (DAP) did not differ significantly from the WT (Figure 2D; Table 1). On the other hand, mutant

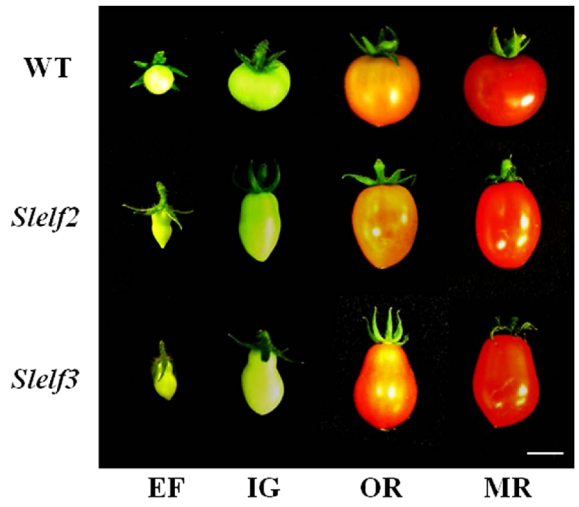

Figure 1. Fruit morphology of Micro-Tom (WT) and mutant lines *Slelf2* and *Slelf3* at early fruit (EF), immature green (IG), orange (OR), and mature red (MR) developmental stages. Scale Bar=1 cm.

plants at 45 DAP were slender, with longer internodes than the controls (Figure 2E); at this stage, plant heights of mutant lines were significantly higher than those of the WT (Table 1).

The noticeable fruit shape elongation caused by *Slelf2* and *Slelf3* mutations began during EF development and continued until the mature red (MR) stage (Figure 1). We measured 15–30 mature red fruits from each line cultivated under our experimental growth conditions. These measurements revealed that the mutations had significant effects on fruit weight, length, and diameter, locule number, and seed number per fruit. In addition, fruits from mutant lines also had higher fruit shape index values (length/width ratios) compared with WT fruit (Table 1).

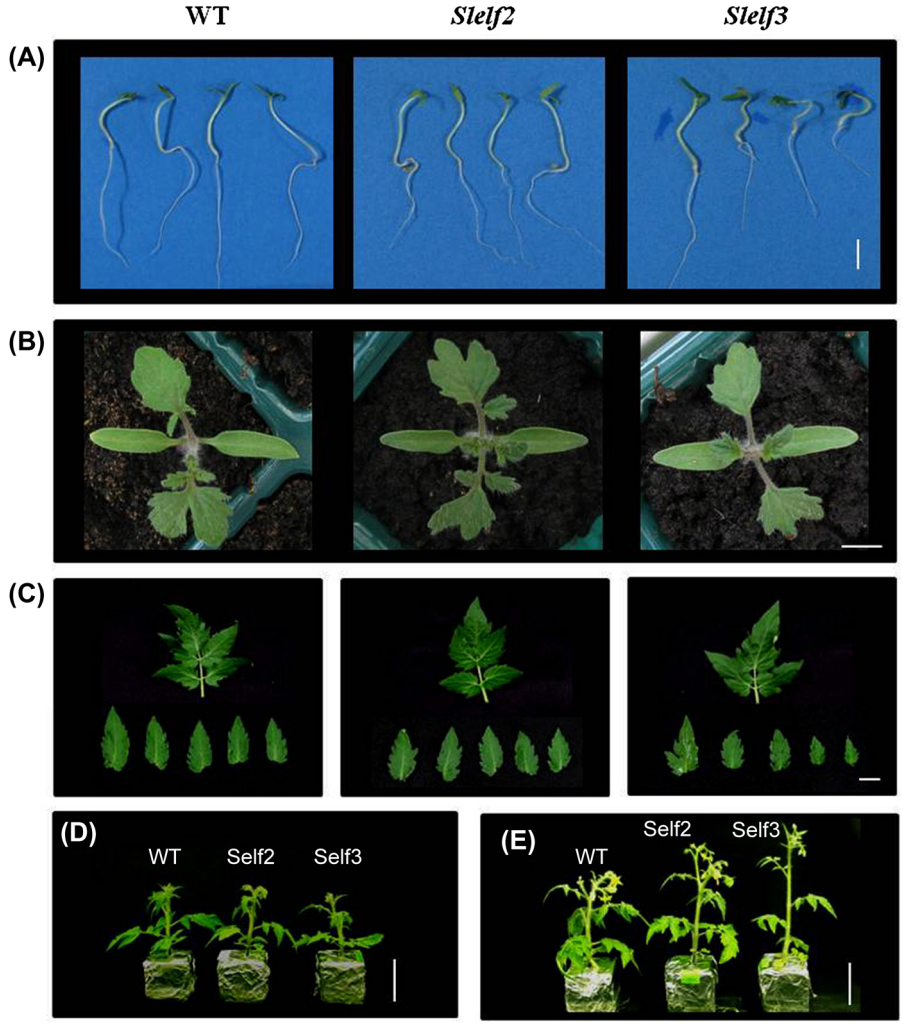

Figure 2. Vegetative morphology of Micro-Tom (WT) and mutant lines *Slelf2* and *Slelf3*. (A) Hypocotyls and roots 7 days after germination. Bar=1 cm. (B) Two-week-old WT, *Slelf2*, and *Slelf3* seedlings. Bar=1 cm. (C) Leaves of WT, *Slelf2*, and *Slelf3* mutant plants. Bar=1 cm. (D and E) Plants of WT and *Slelf2* and *Slelf3* mutant lines at 30 (D) and 45 (E) days after sowing. Bar=5 cm.

Table 1. Phenotypic characterization of vegetative and reproductive structures (mature fruits) of wild-type (WT) Micro-Tom and *Slelf2* and *Slelf3* mutants. Data are means±SE of 4–5 vegetative organs and 15–30 mature fruits. For all measurements, different letters indicate significant differences (Tukey–Kramer HSD test, $p<0.05$). Plants were grown in the greenhouse during the spring of 2012 in Tsukuba, Japan.

Phenotypic character	WT	*Slelf2*	*Slelf3*
Vegetative structures			
Hypocotyl length (cm)	2.31±0.16[a]	2.29±0.13[a]	2.0±0.12[b]
Root length (cm)	5.13±0.38[a]	6.07±0.32[a]	4.71±0.33[b]
Leaf area (mm^2)	25.76±0.7[a]	25.53±0.6[a]	18.93±0.7[b]
Plant height at 30 DAP (cm)	5.36±0.33[a]	4.78±0.30[a]	5.04±0.38[a]
Plant height at 45 DAP (cm)	8.22±0.73[b]	12.25±0.77[a]	12.70±0.68[a]
Reproductive structures			
Fresh weight (g)	5.03±0.11[a]	3.49±0.12[c]	3.76±0.18[c]
Length (mm)	15.6±0.21[b]	18.0±0.32[a]	17.4±0.37[a]
Diameter (mm)	17.9±0.37[a]	14.8±0.28[b]	14.6±0.37[b]
Fruit index	0.85±0.012[b]	1.2±0.018[a]	1.19±0.030[a]
Locule number	3.40±0.10[a]	2.66±0.11[b]	2.60±0.09[b]
Seed number per fruit	21.9±1.3[a]	12.7±0.7[b]	10.9±1.4[b]

Fruit index is a ratio between fruit length and fruit diameter at the widest point.

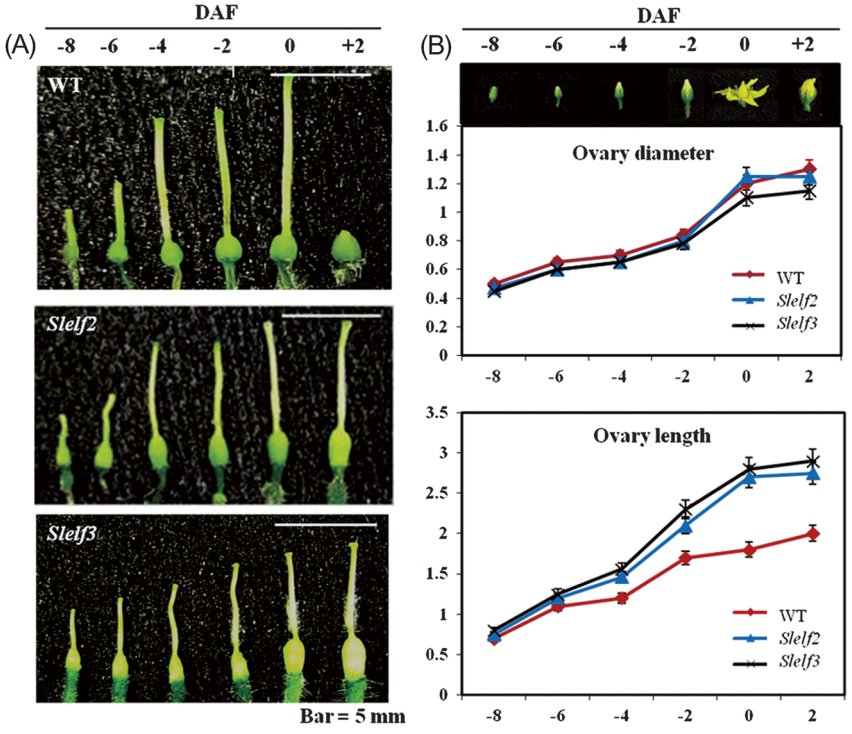

Figure 3. Microscopic analysis of flower bud morphology of Micro-Tom (WT) and mutant lines *Slelf2* and *Slelf3*. (A) Developing pistil at −8, −6, −4, −2, 0, and 2 days after flowering (DAF). Bar=5 mm. (B) Time–course comparison of ovary diameter (upper) and ovary length (lower) at −8, −6, −4, −2, 0, and 2 DAF. Values are means±SE of three ovaries.

Microscopic observation and histological analysis of pistil and fruit formation

The *Slelf2* and *Slelf3* mutations not only induced changes in fruit shape, but also altered ovary morphology. A time-course comparison of pistil development from approximately −8 DAF to 2 DAF in *Slelf2*, *Slelf3* and the WT (Figure 3A) revealed a significantly longer ovary in the WT at approximately −4 DAF, with subsequent expansion in the longitudinal direction (Figure 3B). In contrast, ovary diameters were identical between mutants and the WT. We accordingly conducted a histological analysis of ovary longitudinal sections of mutants and WT at this critical stage (−4 DAF), and also at −8 DAF and 0 DAF (anthesis) (Figure 4A). As indicated by the white arrow in the histograph in Figure 4A, elongation in the *Slelf3* mutant line ovary was primarily limited to the proximal region. The ovary of the *Slelf2* mutant line also displayed an elongated shape, but its proximal region was not predominantly elongated as in *Slelf3*. This result revealed that elongation, particularly in locule tissue, occurred throughout the entire ovary (Figure 4A).

Fruit elongation in *Slelf2* and *Slelf3* could be due to

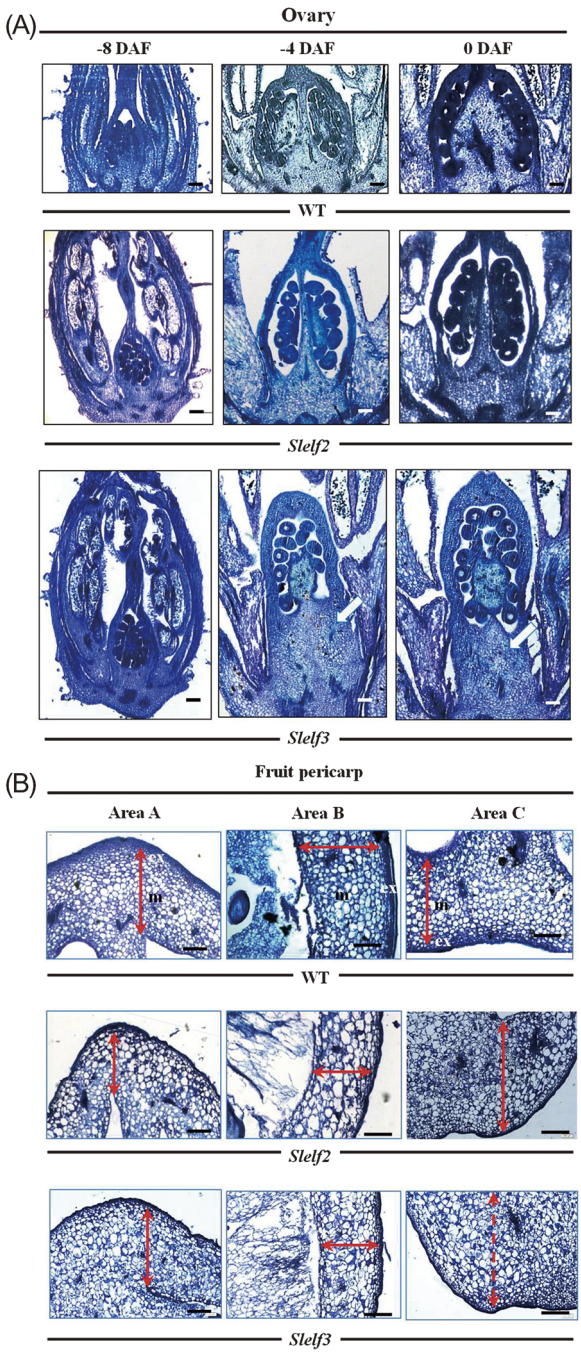

Figure 4. Histological analysis of pistils and fruit pericarps of Micro-Tom (WT) and mutant lines *Slelf2* and *Slelf3*. (A) Longitudinal sections of developing ovaries at −8, −4 and 0 days after flowering (DAF). Bar=100 μm. (B) Longitudinal sections of the pericarp of immature green fruits (10 DAF) from three designated areas: A (distal), B (middle), and C (proximal). Bar=500 μm.

the presence of larger or longer cells, a greater number of cells, or a combination of these factors. Microscopic sections from fruits at 10 DAF were analyzed to determine pericarp thickness and number of cell layers. Quantification of pericarp thickness in fruit distal, middle, and proximal regions (areas A, B, and C respectively of Figure 4B) revealed clear morphological differences in the mesocarp proximal region: this region was much more elongated in *Slelf2* and *Slelf3* fruits than in the WT (Figure 4B and Table 2). In addition to mesocarp thickness differences in the proximal region, a significant increase was noted in the number of cell layers in this region in *Slelf2* and *Slelf3* fruits (Figure 4B and Table 2). In contrast, mesocarp tissue in area B of mutant fruits was significantly reduced compared with the WT (Table 2).

Inheritance pattern of the Slelf3 mutant allele

The mode of inheritance of the genetically encoded elongated fruit shape trait was investigated by crossing the *Slelf3* mutant with WT Micro-Tom and Ailsa Craig cultivars. Segregation in F_2 populations derived from these crosses was scored based on fruit shape index, the ratio of length to diameter at the widest point. Parental-line *Slelf3*, Micro-Tom (WT), and Ailsa Craig fruit shape indices were 1.19, 0.85, and 0.82, respectively, whereas two distinct fruit shapes—round and elongated—were observed in the *Slelf3*×Ailsa Craig F_2 population having respective indices of 0.926 and 1.191 (Tables 1 and 3). As shown by the highly significant *F*-values ($p<0.01$) in Table 3, ANOVA indicated that fruit shape indices of round and elongated fruits were clearly different in both the parental lines and the F_2 population. Consequently, fruit shape index could be used to efficiently distinguish between round and elongated shapes in the F_2 populations. The F_2 population of the *Slelf3*×Ailsa Craig cross was separated into 38 long and 90 round fruits ($\chi^2=1.500$, $p>0.220$), and fruits in the *Slelf3* × Micro-Tom F_2 population were scored as 24 long and 76 round ($\chi^2=0.053$, $p>0.817$). Segregation ratios of F_2 progeny were approximately 1:3 in both Ailsa Craig and Micro-Tom (WT) crosses, suggesting a monogenic recessive inheritance pattern for the *Slelf3* mutant allele (Table 4).

Map position of the Slelf3 mutation

To identify genetic loci controlling fruit shape in *Slelf3*, all 12 tomato chromosomes were mapped in the F_2 population derived from the *Slelf3*×Ailsa Craig cross. Testing of the F_2 progeny in the *Slelf3* mapping population uncovered 38 plants with the mutant phenotype. Based on phenotypic distribution in the F_2 population, we selected 21 individuals showing the most extreme fruit shape index values and used them to construct 30 genetic markers that were mapped onto the 12 chromosomes of the *Slelf3* F_2 population. The *Slelf3* mutation was found to most likely be located between 16797_706 and TES0115 markers on the short arm of chromosome 7 (Figure 5, left). Additional TES markers TES0482, TES0764, TES0054, TES0407, 6700_497, and 4047_436 were used to narrow the map interval containing the mutant allele from 45.2 cM to approximately 0.4 Mb (Figure 5, right). With regard to

Table 2. Comparison of pericarp thickness and number of cell layers in wild-type (WT) Micro-Tom and *Slelf2* and *Slelf3* mutants. Immature green fruits, 10 days after flowering, were used to quantify pericarp thickness and the number of cell layers. Data are means±SE of four fruits. For all measurements, the differences between the WT, *Slelf2*, and *Slelf3* plants were statistically significant (Tukey–Kramer HSD test, $p<0.05$).

Parameter	WT	*Slelf2*	*Slelf3*
Pericarp thickness (mm)			
Exocarp area A (distal)	0.12±0.004[a]	0.11±0.004[a]	0.09±0.010[a]
Exocarp area B (middle)	0.12±0.006[a]	0.09±0.002[ab]	0.08±0.008[b]
Exocarp area C (proximal)	0.14±0.004[a]	0.10±0.005[bc]	0.09±0.007[c]
Mesocarp area A (distal)	1.97±0.19[a]	2.05±0.11[a]	2.27±0.42[a]
Mesocarp area B (middle)	1.83±0.17[a]	1.11±0.12[b]	1.09±0.07[b]
Mesocarp area C (proximal)	2.14±0.28[b]	3.11±0.02[a]	3.74±0.21[a]
Number of cell layers			
Area A (distal)	11.0±1.00[a]	13.0±0.58[a]	12.5±0.50[a]
Area B (middle)	11.0±0.58[a]	9.5±0.96[a]	9.5±0.50[a]
Area C (proximal)	13.0±1.00[b]	16.0±0.82[a]	17.5±0.50[a]

Table 3. Statistical comparisons of fruit index mean values in an *Slelf3*×Ailsa Craig F_2 population and parental lines.

Population	Phenotype	Genotype	Fruit index	*F*	*p*	*n*
P_1	Round	EE	0.850±0.03[a]	659.90**	<0.0001	24
P_2	Long	ee	1.190±0.05[b]			22
F_2	Round	EE/Ee	0.926±0.08[a]	295.91**	<0.0001	90
	Long	ee	1.191±0.07[b]			38

Abbreviations: P_1, parent 1 (Ailsa Craig [AC]); P_2, parent 2 (*Slelf3*); WW, homozygous genotype for the AC allele; Ws, heterozygous genotype; ss, homozygous genotype for the *Slelf3* allele; *n*, number of plants per genotypic class. Fruit index is a ratio between fruit length and fruit diameter at the widest point. Different letters indicate significant differences between means (*t*-test, $p<0.05$). *F*- and *p*-values were calculated by single one-way ANOVA; ** significant at $p<0.01$.

Table 4. Inheritance pattern of *Slelf3* mutant alleles.

Population[a]	F_2 segregation[b] (mutant : WT)	χ^2[c]	*p*[c]	Inheritance pattern[d]
Slelf3×Ailsa Craig (F_2)	38 : 90	1.500	0.220	monogenic recessive
Slelf3×Micro-Tom (F_2)	24 : 76	0.053	0.817	monogenic recessive

[a] *Slelf* mutants were crossed with wild-type (WT) Micro-Tom and Ailsa Craig. [b] The number of progeny exhibiting the WT (round fruit) or mutant (long fruit) phenotype in each F_2 population is shown. [c] χ^2- and *p*-values were calculated for the F_2 populations. [d] Inheritance pattern was estimated based on the χ^2 value. Values were considered significant if $p<0.05$.

TES0407 and 6700_497 markers, genotypic analysis revealed that 18 out of 21 F_2 progeny with elongated fruit phenotypes possessed Micro-Tom alleles.

Effect of the Slelf3 mutation on transcript levels of cell division- and expansion-related genes

To support the histological data, we extracted total RNA from ovaries, fruit pericarps, cotyledons, stems, sepals, petals, and anthers to analyze transcript levels of genes involved in cell division and expansion. For fruit pericarps, expression levels in the three areas from the microscopic analysis were analyzed. The results of the qRT-PCR expression analysis are shown in Figure 6. mRNA levels of the cell-cycle gene *SlCDKB2.1* increased after pollination, and then decreased during the later stages of fruit development. *SlCDKB2.1* expression was much higher in the mutant line than in the WT, and was correlated with ovary and fruit development. The highest expression was detected at 4 DAF, predominantly in the fruit proximal region (area C). Maximum expression of the mutant line was more than 50% of that found at a similar stage in the WT (Figure 6A). *Slelf3* transcript levels of *SlEXPA5*, a cell expansion-related gene encoding an expansin precursor, also increased after pollination, but were lower than in the WT. At 10 DAF in the fruit proximal region (area C), however, expression was much higher in *Slelf3* than in the WT (Figure 6B).

Discussion

In this study, we characterized *Slelf2* and *Slelf3* mutants in the background of Micro-Tom, a semi-dwarf tomato variety with round fruits. These two EMS-induced mutants exhibited an elongated fruit shape and elongated pistils, the latter observation based on a time-course comparison of pistil development that revealed a predominantly long shape at −4 DAF (Figures 3 and 4A). Histological observation revealed that the elongated ovary shape of *Slelf2* at −4 and 0 DAF was due to longitudinal expansion, whereas the *Slelf3* ovary was greatly altered in the proximal region (Figure 4A). Over-expression of *SUN* reportedly stimulates ovary elongation and is positively correlated with slender phenotypes in cotyledons, leaflets, and floral organs (Wu et al. 2011).

In addition, the effects of increased *SUN* expression after pollination can be observed in developing fruit at 5 DAF, which corresponds to the cell division stage of fruit development (van der Knaap and Tanksley 2001; Xiao et al. 2009).

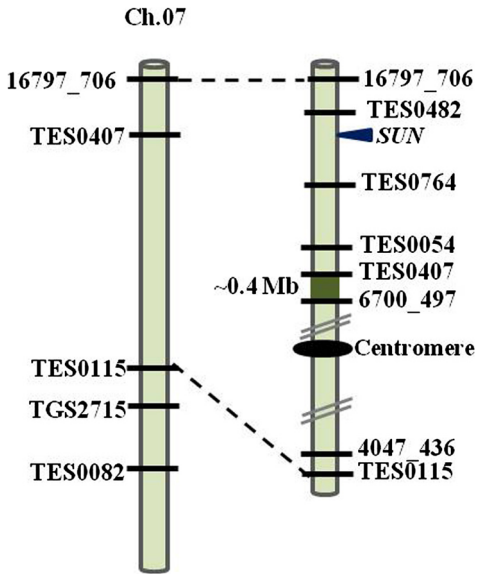

Figure 5. Chromosomal position of the *Slelf3* mutation. Rough maps were generated using SSR, CAPs, and dCAPs markers. The *Slelf3* candidate gene is located on the short arm of chromosome 7. Genetic distances are expressed in megabase pair (Mb).

The *Slelf2* and *Slelf3* mutations were analyzed for their roles in controlling long fruit shape. During examination of the morphology of vegetative and fruit formation, we noted that the *Slelf2* mutation affected fruit structures by significantly influencing fresh weight, fruit length, fruit diameter, locule number, and seed number per fruit, but did not alter vegetative structures, with the exception of plant height at 45 DAP. In contrast, the mutation in *Slelf3* stimulated all plant architecture parameters, except for plant height at 30 DAP (Table 1). The *Slelf2* and *Slelf3* mutations promoted longitudinal growth, decreased horizontal growth, and reduced the number of locules, and accordingly diminished seed numbers per fruit. In addition to altered fruit formation, *Slelf3* decreased leaf area, increased height at 45 DAP, and reduced leaf lobing; these phenotypic effects are very similar to the increased height and reduced leaf lobing reported in a *DELLA* mutant due to its constitutive GA expression (Carvalho et al. 2011). To gain deeper insight into possible roles of GA regulation, however, an expression analysis of GA response genes in plant tissues is needed.

Based on fruit shape, tomatoes have been classified into eight categories (IPGRI 1996; UPOV 2001). In a study of the evolution of fruit shape diversity, the allele distribution of *SUN, OVATE, LC* (*LOCULE NUMBER*), and *FAS* (*FASCIATED*) genes was strongly correlated

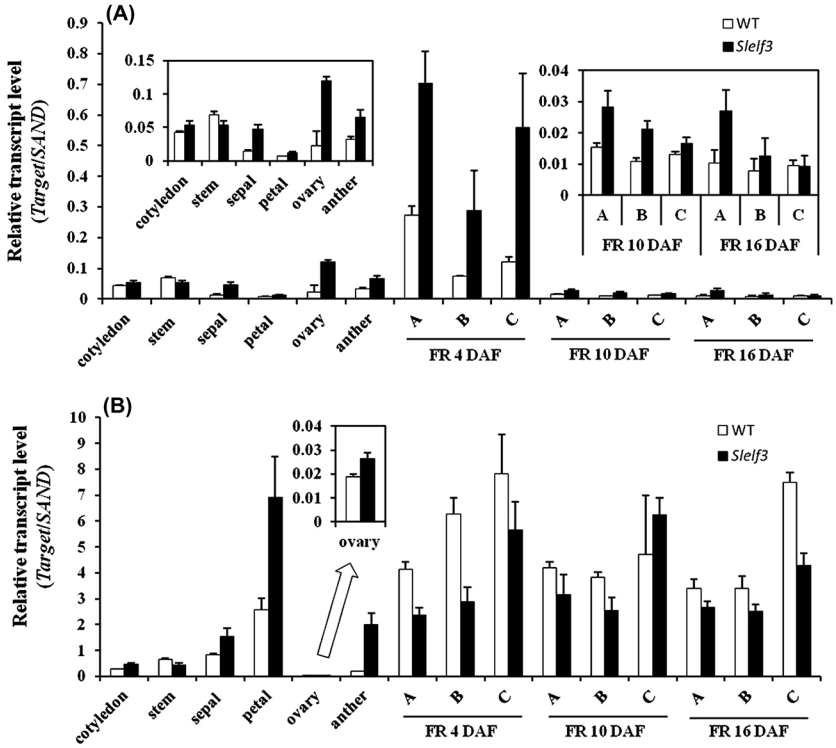

Figure 6. Transcript levels of cell cycle- and cell division–related genes in developing wild-type (WT) Micro-Tom and the *Slelf3* mutant. (A) Relative transcript levels of cell-cycle gene *SlCDKB2.1* in cotyledons, stems, sepals, petals, ovaries, anthers, and developing fruits at 4, 10, and 10 days after flowering (DAF). (B) Relative transcript levels of a cell-expansion gene encoding an expansin precursor (*SlEXPA5*). The values indicate the mean and standard diviation (n=3).

with the UPOV and IPGRI fruit shape classifications (Rodriguez et al. 2011). In our study, genetic analysis of *Slelf2* demonstrated incomplete dominant, whereas *Slelf1* and *Slelf3* revealed recessive alleles. Furthermore, to understand the gene that contributed to *Slelf1* and *Slelf3* mutations are alleles of one gene or of different genes, we performed the allelism test and the result of intercrossing mutants demonstrated round fruit phenotype (wild-type phenotype) suggesting that these two mutants are complement and caused by a mutant allele of difference gene (allele). Rough Mapping of the *Slelf3* mutant was accomplished using the Tomato-EXPEN 2000 map along with a combination of SSR, CAPs, and dCAPs markers (Shirasawa et al. 2010). The *Slelf3* candidate gene was localized within an approximately 0.4-Mb region on the short arm of chromosome 7 (Figure 5). Genome-wide identification of *SUN* and *OVATE*-like gene families has demonstrated that *SlSUN* (*Solanum lycopersicum* SUN-like protein) and *SlOFP* (*Solanum lycopersicum* OVATE family protein) genes are enriched on the top and bottom segments of several chromosome and have originated from a tandem duplication event. Nevertheless, OVATE family protein genes have not currently been identified on the short arm of chromosome 7 (Huang et al. 2013). On the other hand, a *Rider* retrotransposon-mediated duplication of a 24.7-kb *SUN* fragment, associated with fruit elongation in several tomato cultivars, has been located on the short arm of chromosome 7 (Jiang et al. 2009; Xiao et al. 2008). As shown in Figure 5, however, its physical position differs from that of the *Slelf3* mutation. Consequently, the causal gene controlling *Slelf3* mutant fruit elongation is likely different from previously known loci affecting fruit shape.

To analyze the manner in which *Slelf2* and *Slelf3* mutations regulate elongated fruit development, we performed histological and expression analyses. Tomato fruit is composed of different tissues: the pericarp (flesh)—subdivided into exocarp, mesocarp, and endocarp, and the placenta, septum, and locules, the latter filled with jelly and seeds (Bertin 2005; Mintz-Oron et al. 2008). Tomato fruit organogenesis is influenced by the relationship between cell division and cell expansion, two processes that respectively determine fruit cell number and relative cell size (Chevalier et al. 2011). Histological analysis revealed that fruit pericarp thickness and the number of cell layers were mainly increased in the proximal region (area C) (Figure 4B), although the pericarp in area B displayed a reduction in thickness but no alteration in the number of cell layers between WT and mutant lines (Table 2). To support the histological data, qRT-PCR-based expression analysis of genes involved in cell division and expansion were performed. Cyclin-dependent protein kinases (CDKs) are major regulators of cell cycle progression and play a crucial controlling role in cell division (Inze and De Veylder 2006). *SlCDKB2* is predominant expressed in the pericarp during the early developmental stages, when mainly cell division takes place and decrease gradually during later stages till completely abolished at the mature green stage (Czerednik et al. 2012; Joubes et al. 2001). On the other hand, *SlEXPA5*, the cell expansion-related gene encoding for an expansin precursor increased after pollination (Vriezen et al. 2008). Our study showed that expression of the *SlCDKB2.1* cell-cycle gene was higher in the ovary and fruit pericarp of the *Slelf3* mutant compared with the WT, particularly in the proximal region (area C) of the fruit pericarp (Figure 6A). *SlCDKB2* is primarily expressed in the pericarp during early developmental stages when cell division predominates, with gradually decreased expression in later stages and complete cessation at the mature green stage (Czerednik et al. 2012; Joubes et al. 2001). We also found that mRNA levels of *SlEXPA5* increased after pollination (Figure 6B), confirming the results of Vriezen et al. (2008). In an earlier study, mRNA transcripts of this gene were detected in expanding fruit, but were most abundant in full-size, maturing green fruit and declined during early ripening stages (Brummell et al. 1999). In our study, *SlEXPA5* mRNA levels in the *Slelf3* mutant were generally lower than in the WT, with comparable levels observed in fruit pericarps from 4 DAF to 16 DAF. Moreover, to understand significantly overrepresented function categories in cell division activity in elongated fruit phenotype, comparison of the global pattern of gene expression and hormone response would be deliberate. The other cell division- and expansion-related genes for instant *SlCycB1.1* cell-cycle gene, *SlPec*-cell expansion related gene-encoding for a pectatelyase and an endo-xyloglucan transferase (*SlXTH1*) as well as the other plant hormone such as gibberellin are considered to breakdown the kind of proteins encode the *Slelf3* mutant.

In summary, the mutations present in *Slelf2* and *Slelf3* lines resulted in elongated ovary and fruit phenotypes. Ovary elongation in the *Slelf2* mutant was verified to occur not only in the proximal region, but throughout, especially in the locule tissue. In the *Slelf3* mutant, in contrast, several pieces of evidence demonstrate that expansion in flower buds and fruit at 10 DAF occurred primarily in the proximal region (area C). Transcript level analysis of cell division- and expansion-related genes suggested that the mutation most likely regulated cell division activity, with maximum expression in fruit occurring at 4 DAF predominantly in the proximal region (area C). Finally, our results related to the *Slelf3* mutant clearly contribute to the fine mapping and elucidation of the casual genes controlling elongated fruit shape in tomato.

Acknowledgements

The authors thank the National BioResearch Project (NBRP), MEXT, Japan for providing the Seeds of *S. lycopersicum* cv. Micro-Tom, TOMJPE2407 and TOMJPE839 (NBRP-tomato, http://tomato.nbrp.jp/indexEn.html) from the TOMATOMA database (http://tomatoma.nbrp.jp/). We also thank all members of Prof. Hiroshi Ezura laboratory for helpful discussions throughout the work.

References

Andersen SU, Buechel S, Zhao Z, Ljung K, Novak O, Busch W, Schuster C, Lohmann JU (2008) Requirement of B2-type cyclin-dependent kinases for meristem integrity in *Arabidopsis thaliana*. *Plant Cell* 20: 80–100

Bertin N (2005) Analysis of the tomato fruit growth response to temperature and plant fruit load in relation to cell division, cell expansion and DNA endoreduplication. *Ann Bot* (Lond) 95: 439–447

Brummell DA, Harpster MH, Dunsmuir P (1999) Differential expression of expansin gene family members during growth and ripening of tomato fruit. *Plant Mol Biol* 39: 161–169

Carvalho RF, Campos ML, Pino LE, Crestana SL, Zsögön A, Lima JE, Benedito VA, Peres LEP (2011) Convergence of developmental mutants into a single tomato model system: 'Micro-Tom' as an effective toolkit for plant development research. *Plant Methods* 7: 18

Chevalier C (2007) Cell cycle control and fruit development. *Ann Plant Rev* 32: 269–290

Chevalier C, Nafati M, Mathieu-Rivet E, Bourdon M, Frangne N, Cheniclet C, Renaudin JP, Gevaudant F, Hernould M (2011) Elucidation the function role of endoreduplication in tomato fruit development. *Ann Bot* (Lond) 107: 1159–1169

Czerednik A, Busscher M, Bielen BAM, Wolters-Arts M, de Maagd RA, Angenent GC (2012) Regulation of tomato fruit pericarp development by an interplay between *CDKB* and *CDKA1* cell cycle genes. *J Exp Bot* 63: 2605–2617

Huang Z, Van Houten J, Gonzalez G, Xiao H, van der Knaap E (2013) Genome-wide identification, phylogeny and expression analysis of *SUN*, *OFP* and *YABBY* gene family in tomato. *Mol Genet Genomics* 288: 111–129

Inze D, De Veylder L (2006) Cell cycle regulation in plant development. *Annu Rev Genet* 40: 77–105

IPGRI (1996) *Descriptors for Tomato* (*Lycopersicon* spp.). International Plant Genetic Resources Institute, Rome

Jiang N, Gao D, Xiao H, van der Knaap E (2009) Genome organization of the tomato *sun* locus and characterization of the unusual retrotransposon *Rider*. *Plant J* 60: 181–193

Joubes J, Lemaire-Chamley M, Delmas F, Walter J, Hernould M, Mouras A, Raymond P, Chevalier C (2001) A new C-type cyclin-dependent kinase from tomato expressed in dividing tissues does not interact with mitotic and G_1 cyclins. *Plant Physiol* 126: 1403–1415

Liu J, Van Eck J, Cong B, Tanksley SD (2002) A new class of regulatory genes underlying the cause of pear-shape tomato fruit. *Proc Natl Acad Sci USA* 99: 13302–13306

Mintz-Oron S, Mandel T, Rogachev I, Feldberg L, Lotan O, Yativ M, Wang Z, Jetter R, Venger I, Adato A, et al. (2008) Gene expression and metabolism in tomato fruit surface tissues. *Plant Physiol* 147: 823–851

Mueller LA, Solow TH, Taylor N, Skwarecki B, Buels R, Binns J, Lin C, Wright MH, Ahrens R, Wang Y, et al. (2005) The SOL Genomics Network: a comparative resource for Solanaceae biology and beyond. *Plant Physiol* 138: 1310–1317

Rodriguez ME, Borges AA, Perez AB, Perez JA (2008) Selection of internal control genes for quantitative real-time RT-PCR studies during tomato development process. *Plant Biol* 8: 131–142

Rodriguez GR, Munos S, Anderson C, Sim SC, Michel A, Causse M, Gardener BB, Francis D, van der Knaap E (2011) Distribution of *SUN*, *OVATE*, *LC*, and *FAS* in the Tomato Germplasm and the Relationship to Fruit Shape Diversity. *Plant Physiol* 156: 275–285

Saito T, Ariizumi T, Okabe Y, Asamizu E, Hiwasa-Tanase K, Fukuda N, Mizoguchi T, Yamasaki Y, Aoki K, Ezura H (2011) TOMATOMA: a novel tomato mutant database distributing Micro-Tom mutant collections. *Plant Cell Physiol* 52: 283–296

Sampedro J, Cosgrove DJ (2005) The expansin superfamily. *Genome Biol* 242: 1–11

Shirasawa K, Asamizu E, Fukuoka H, Ohyama A, Sato S, Nakamura Y, Tabata S, Sasamoto S, Wada T, Kishida Y, et al. (2010) An interspecific linkage map of SSR and intronic polymorphism markers in tomato. *Theor Appl Genet* 121: 731–739

UPOV (2001) *Guidelines for the Conduct of Tests for Distinctness, Uniformity and Stability (Tomato)*. Geneva

van der Knaap E, Tanksley SD (2001) Identification and characterization of a novel locus controlling early fruit development in tomato. *Theor Appl Genet* 103: 353–358

Vriezen WH, Feron R, Maretto F, Keijman J, Mariani C (2008) Change in tomato ovary transcriptome demonstrate complex hormonal regulation of fruit set. *New Phytol* 177: 60–76

Wu S, Xiao H, Cabrera A, Meulia T, van der Knaap E (2011) *SUN* regulates vegetative and reproductive organ shape by changing cell division patterns. *Plant Physiol* 157: 1175–1186

Xiao H, Jiang N, Schaffner EK, Stockinger EJ, van der Knaap E (2008) A retrotranspson-mediated gene duplication underlines morphologenesis. *Plant Cell* 17: 2676–2692

Xiao H, Radovich C, Welty N, Hsu J, Li D, Meulia T, van der Knaap E (2009) Integration of tomato reproductive developmental landmarks and expression profiles, and the effect of *SUN* on fruit shape. *BMC Plant Biol* 9: 49

Yamamoto N, Tsugane T, Watanabe M, Yano K, Maeda F, Kuwata C, Torki M, Ban Y, Nishimura S, Shibata D (2005) Expressed sequence tags from the laboratory-grown miniature tomato (*Lycopersicon esculentum*) cultivar Micro-Tom and mining for single nucleotide polymorphisms and insertions/deletions in tomato cultivars. *Gene* 356: 127–134